

Three-dimensional off-lattice model for the interface growth of polycrystalline materials

E. V. Albano, R. C. Salvarezza, L. Vázquez,* and A. J. Arvia

Instituto de Investigaciones Fisicoquímicas Teóricas y Aplicadas (INIFTA), Sucursal 4, Casilla de Correo 16, (1900) La Plata, Argentina

(Received 29 October 1998)

A three-dimensional off-lattice model is developed to explain the interface evolution of polycrystalline materials grown under surface reaction control. The model includes random deposition and surface diffusion of depositing particles with energy barriers located at step edges and crystal boundaries. Depending on the height of the barriers existing at step edges and crystal boundaries, this model predicts either a scale-dependent or a scale-independent value of the growth exponent (β). Scale-dependent values of β reported for polycrystalline films grown under surface reaction control can be explained by the proposed model. [S0163-1829(99)02708-3]

In recent years there has been increasing interest in developing both continuum and discrete models for the interface evolution of solid films.¹ These models are interesting to understand the morphology evolution of real solid films that is strongly determined by the relative contribution of different physical processes. The properties of solid films such as optical reflectivity, porosity, and conductivity depend on their structure and morphology. In general, models include the stochastic noise related to the growth process and surface relaxation through either surface diffusion or surface tension. Most frequently, growth models have dealt with monocrystalline phases and homoepitaxial growth,¹ whereas real films that can be produced by different techniques such as chemical vapor deposition (CVD), electrodeposition (ED), evaporation (EV), and sputtering (SP) are usually polycrystalline materials. Therefore, theoretical models for describing the interface evolution at polycrystalline films are welcome.

The interface evolution of solid films has been studied mainly within the framework of the dynamic scaling theory² and applied to both single-crystal and polycrystalline surfaces growing under surface reaction control.^{1,3} The dynamic scaling theory predicts that for a substrate of size L the interface width, $w(L,t)$, increases with time according to $w(L) \propto t^\beta$ for $t \rightarrow 0$, whereas $w(L)$ is constant for $t \rightarrow \infty$, i.e., the interface width reaches saturation.² Furthermore, the correlation length ξ increases with time as $\xi \propto t^{1/z}$, β , z , and $1/z$ being the growth, dynamic, and coarsening exponents, respectively.

Experimental studies on the growth of polycrystalline solids have shown that β becomes scale-dependent.^{4,5} In some cases, values in the range $0.25 \leq \beta \leq 0.3$ have been observed for length scales smaller than the average crystal size $L_c(t)$, a time-dependent parameter that plays the role of ξ , whereas higher values of β have been found for $L > L_c(t)$. In other cases, $w(L,t)$ reaches saturation for $L > L_c$, and only a single value of β in the range $0.2 \leq \beta \leq 0.4$ has been obtained.^{3,6,7} For single-crystal growth, $\beta > 0.3$ has been assigned to the presence of step-edge energy barriers that hinders surface diffusion of depositing particles.¹ Conversely, the role played by these barriers in the interface evolution of polycrystalline films has been questioned because of ill-defined steps at crystal surfaces.³ However, this situation becomes more complex as occasionally crystals at polycrystalline films exhibit well-defined monatomic high steps.

Therefore, the role of step-edge energy barriers at these films should be revisited and further explored.

A first attempt to model the growth of polycrystalline films was made by Van der Drift (VDD).⁸ The VDD model predicts $1/z \approx 0.4$ and neglects correlations among crystals and stochastic fluctuations in crystal size during growth. In this paper, a new three-dimensional (3D) off-lattice model for the random growth of these films under surface reaction control including step-edge and crystal-boundary energy barriers for the transport of depositing particles along the surface is presented. Results from the model allow us to discuss recent data on the scaling behavior of polycrystalline films grown by SP,³ EV,^{4,6} ED,⁵ and CVD.⁷ The scaling behavior of these films could not be fully explained by the existing growth models. The proposed model predicts either one or two values of β (for $L < L_c$ and $L > L_c$) depending on the heights of the step-edge energy barrier and crystal-boundary energy barrier. Since this work is an attempt to model the interface evolution of polycrystalline films, it aims to provide a qualitative rather than a quantitative description of the scaling behaviors experimentally observed.

The growth process is simulated on a two-dimensional (2D) off-lattice flat substrate of dimension side M with periodic boundary conditions. Initially a fixed density, ρ_0 , of randomly distributed nucleation centers on the substrate is considered. At the submonolayer regime, crystal growth proceeds at these centers through the peripheral capture of surface diffusing particles. As these crystals are randomly oriented in the off-lattice substrate, the formation of intercrystalline gaps (crystal boundaries) occurs. After monolayer completion, crystal growth proceeds according to a generalization of the rules for random deposition with relaxation to the nearest-neighbor sites (surface diffusion^{9,10}) preventing overhang formation. Thus, depositing particles are selected at random in the off-lattice substrate and drop onto the nearest occupied site. Deposited particles are allowed to relax to the nearest-neighbor site of lower height with a probability P_e jumping from an upper to a lower neighbor terrace (step-edge barriers).¹¹ For $P_e = 0$, interlayer mass transport is hindered completely by step-edge energy barriers, whereas for $P_e = 1$ it is permitted inside each crystal. Particles impinging at higher crystal boundaries are allowed to relax, either becoming attached to the same crystal with the probability P_s or stuck on top of lower neighbor crystals with the intercrystal mass transport probability P

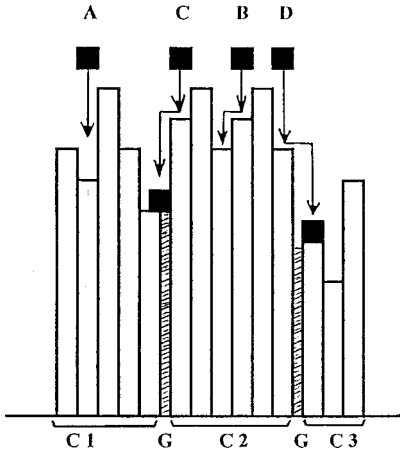


FIG. 1. Sketch of three crystals ($C1$, $C2$, and $C3$) and two intercrystalline gaps (G), which shows the different processes that an incoming particle can undergo. It can be deposited directly without relaxation (A) or after surface diffusion relaxation to a next lower neighbor site of the same crystal (B). If a particle reaches the intercrystalline gap (G), two different processes can occur: either the particle is attached to the higher crystal with probability P_s (C) or it is attached to the next neighbor lower crystal with probability $P = 1 - P_s$ (D).

$= 1 - P_s$. Possible interfacial processes for the incoming particle as described by the model are sketched in Fig. 1.

Simulations were performed for $M = 50$, $0.05 \leq \rho_0 \leq 0.20$, $0.01 \leq P_e \leq 1$, $0 \leq P \leq 0.95$, and films growing up to 2×10^4 layers. Results were averaged over 50–400 different realizations.

Sequential top-view snapshots resulting from this model for $P = 0$ and $P_e = 1$ show a coarsening of deposited crystals [Figs. 2(a) and 2(b)]. As advanced stages of growth, the 3D image reveals crystals of different heights with smooth top surfaces and crystal boundaries [Fig. 2(c)]. The smooth topography arises from surface diffusion in the absence of step-edge barriers¹ for impinging particles ($P_e = 1$). Conversely, crystal coarsening results from intercrystal boundary energy barriers that prevent the overlap of growing crystals ($P = 0$), leading to an increasing population of buried crystals. The probability of a crystal surviving, P_{sur} , at time t in the asymptotic regime fits a power-law behavior $P_{\text{sur}}(t) \propto t^{-p}$.^{12,13} Accordingly, the relationships $P_{\text{sur}}(t) \propto t^{-p} \propto N_c(t) \propto [L_c(t)]^{-2} \propto t^{-2/z}$ are derived, $N_c(t)$ being the crystal density. Assuming that $h \propto t$, the height distribution function of crystals, $D(h)$, obtained from the derivative of $P(t)$, yields $D(h) \propto h^{-(1+2/z)}$. The slope of $\log_{10} D(h)$ versus $\log_{10} h$ plots gives $1 + 2/z \approx 1.76 \pm 0.02$ and $1/z = 0.38$ [Fig. 3(a)]. It should be noted that the crystal height distribution function indicates buried crystals of all heights, that is, the height distribution shows scale invariance. We also calculate $L_c(t)$ from the number of crystals/deposit area ratio, resulting in $L_c \propto h^{1/z}$ with $1/z \approx 0.33 \pm 0.02$ [Fig. 3(b)], in reasonable agreement with $1/z$ obtained from the $D(h)$. These exponents remain unchanged within error bars for $0 \leq P \leq 0.9$, but for $P > 0.9$ they decrease to attain $1/z = 0.27$ (Table I). For $P = 0.5$ and P_e decreasing from 0.1 to 0.01, a sharp decrease in $1/z$ results [Fig. 3(b) and Table I].

Values of β as a function of P and P_e for both intracrystal

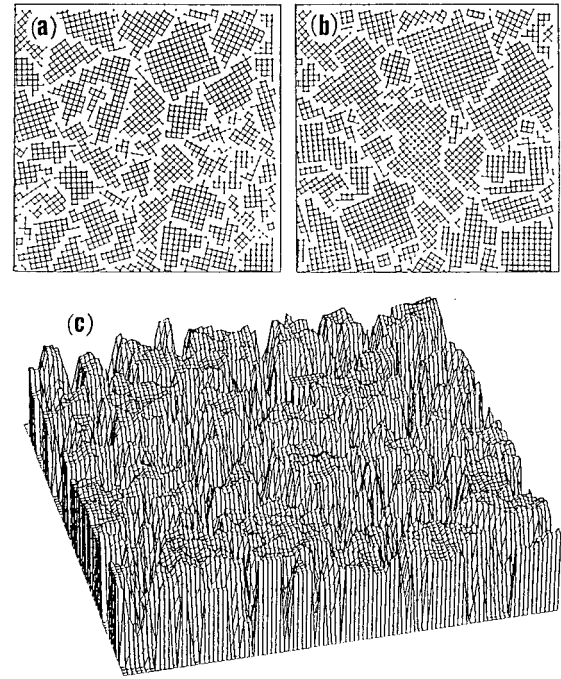


FIG. 2. Typical top-view snapshots resulting from the model at different growing stages showing crystal coarsening for $P_e = 1$ and $P = 0$. (a) Top view of the first layer with 50 crystals, (b) top view of the sample after deposition of 100 layers, on average, with 32 crystals, (c) 3D snapshot obtained after deposition of 100 layers.

(β_c) and intercrystal transport (β_{ic}) (Table I) were evaluated from $\log_{10}[w(L)]^2$ versus $\log_{10} h$ plots [Fig. 3(b) inset] for $L < L_c$ and $L > L_c$, respectively. In the first case, $w(L, t)$ was measured for each crystal surface and averaged over the total number of deposited crystals. In the second case, $w(L, t)$ was measured for the whole deposit surface.

For $L < L_c$ and $P_e = 1$, $\beta_c \approx 0.2$, irrespective of P (Table I), as has been reported for random deposition models where surface diffusion is dominant.¹ In our model the addition of step-edge energy barriers to the simple surface diffusion mechanism increases β_c .^{1,11} Thus, for $P = 0.5$, β_c changes from 0.2 to 0.48 as P_e is decreased from 1 to 0.01. The value $\beta_c \approx 0.5$ has been reported for single-crystal surfaces when the transport of particles at steps is hindered.^{1,11}

For $L > L_c$, β_{ic} also depends on P and P_e . Thus, when $P_e = 1$ and $P = 0$, $\beta_{ic} \approx 0.52$. This means that each crystal grows independently. For a constant P_e , as P is increased from 0 to 0.95, β_{ic} decreases approaching β_c . In this case, the efficient surface transport of particles between growing crystals leads to a smooth deposit.

For $P = 0.5$, the change in P_e from 1 to 0.01 leads to an increase in β_{ic} from 0.33 to 0.45, that is, $\beta_{ic} \rightarrow \beta_c$. The high value of β_c is due to the contribution of the step-edge energy barriers.

Our growth model for polycrystalline materials predicts scale-dependent β values depending on the heights of the step-edge energy barrier and crystal-boundary energy barrier. Let us consider recent scaling data from STM imaging, that is, for Au-EV films, $\beta_c = 0.25 \pm 0.06$, $\beta_{ic} = 0.45 \pm 0.05$, and $1/z = 0.24$,⁴ and for Au-ED films, $\beta_c = 0.31 \pm 0.08$, $\beta_{ic} = 0.49 \pm 0.05$, and $1/z = 0.33$.⁵ According to our model, the fact that $\beta_{ic} > \beta_c$ implies that crystal boundary barriers are

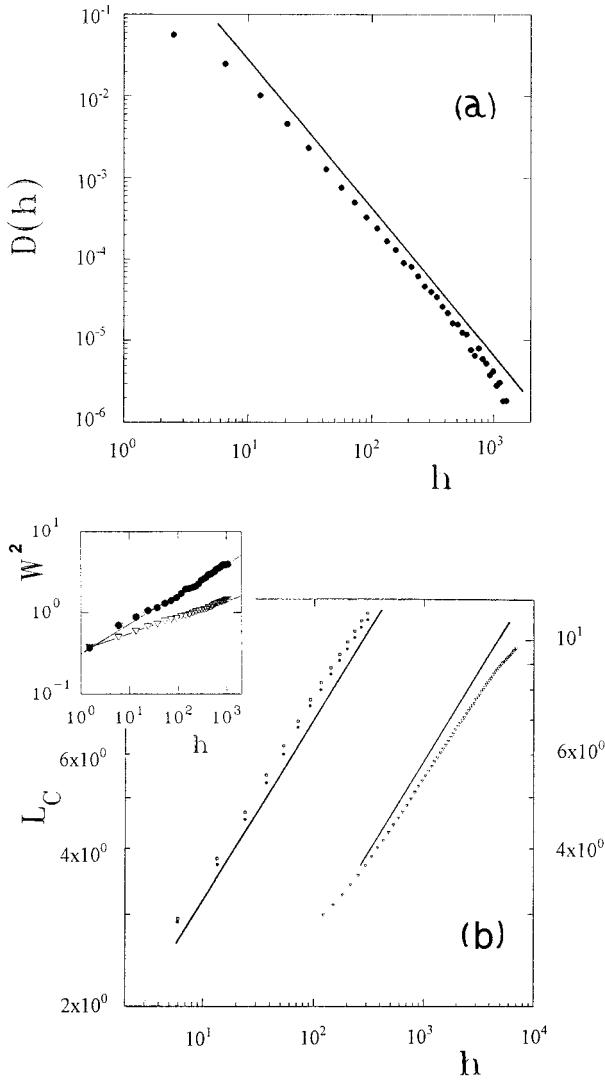


FIG. 3. (a) Logarithmic plots of the distribution of the heights of buried crystals $D(h)$ versus the average film thickness h for $P_e = 1$ and $P = 0$. The straight line with slope $1 + 2/z = 1.76$ has been drawn as a visual guide. (b) Logarithmic plots for the average crystal size L_c vs h for $P_e = 1$ and $P = 0$ (\circ); $P_e = 1$ and $P = 0.5$ (\bullet); $P_e = 0.10$ and $P = 0.50$ (∇). Straight lines with slopes $1/z = 0.35$ have been drawn as a visual guide. The inset shows logarithmic plots of w^2 vs h for $P_e = 1$ and $P = 0.5$; (∇) crystal interface width; (\bullet) intercrystal interface width. Straight lines with slopes $2\beta_c = 0.66$ and $2\beta_{ic} = 0.36$ are drawn.

higher than those at step edges. Therefore, barriers at crystal boundaries determine the evolution of $w(L, t)$ at $L > L_c$. Otherwise, step-edge barriers that determine $w(L, t)$ at $L < L_c$ cannot be completely neglected as β_c becomes greater than $\beta_c \approx 0.2$, as predicted by surface diffusion without step-edge energy barrier. In fact, non-negligible step-edge energy barriers¹⁴ are responsible for the departure from a perfect 2D morphology in Au(111)-ED crystals.¹⁵

Conversely, for Pt-SP, $\beta_c = 0.26$, $\beta_{ic} \approx \beta_c$, and $1/z \approx 0.28$.³ According to our model these figures indicate low step-edge barriers with an efficient intercrystal mass transport. For Ag-EV films [$\beta_c = 0.29$, $\beta_{ic} \approx \beta_c$, and $1/z = 0.40$ (Ref. 6)] and W-CVD films [$\beta_c = 0.37 \pm 0.06$, $\beta_{ic} \approx \beta_c$, and $1/z = 0.40$ (Ref. 7)], step-edge energy barriers become more

TABLE I. Values of β_c (intracrystal growth exponent), β_{ic} (intercrystals growth exponent), and $1/z$ obtained from our model for $\rho_0 = 0.20$ and $N_c = 500$, and different values of P and P_e .

P_e	P	β_c	β_{ic}	$1/z$
1	0	0.17 ± 0.05	0.52 ± 0.07	0.33 ± 0.03
1	0.1	0.18 ± 0.05	0.35 ± 0.05	0.32 ± 0.03
1	0.5	0.18 ± 0.05	0.33 ± 0.05	0.35 ± 0.03
1	0.6	0.17 ± 0.05	0.29 ± 0.05	0.33 ± 0.03
1	0.8	0.20 ± 0.05	0.27 ± 0.05	0.32 ± 0.03
1	0.9	0.19 ± 0.05	0.28 ± 0.05	0.30 ± 0.03
1	0.95	0.19 ± 0.05	0.26 ± 0.05	0.27 ± 0.03
0.1	0.5	0.24 ± 0.05	0.29 ± 0.05	0.28 ± 0.02
0.05	0.5	0.37 ± 0.05	0.38 ± 0.05	
0.05	0.05	0.35 ± 0.03	0.38 ± 0.01	0.10 ± 0.02
0.05	0.01	0.35 ± 0.03	0.38 ± 0.01	0.10 ± 0.02
0.01	0.5	0.48 ± 0.05	0.45 ± 0.05	

significant than barriers operating at crystal boundaries. Note that in all these cases $w(L, t)$ is dominated by the step-edge barrier so that it saturates for $L > L_c$.

Finally, for negligible step-edge energy barriers ($P_s = 1$) the following scenario can be advanced. Each crystal involves a smooth surface and $\beta \approx 0.2$ in agreement with the predictions of surface diffusion models for interface evolution.^{9,10} These models also predict $0.20 \leq 1/z \leq 0.25$ as observed in our model when an unrestricted intercrystal mass transport takes place (Table I). Conversely, for $P \rightarrow 0$, $0.33 \leq 1/z \leq 0.35$ is close to the predictions of the model of Yao and Guo.¹⁶ However, in our surface reaction controlled model shadowing is much less important, apart from events at intercrystalline gaps, than in Ref. 16, where particles deposit ballistically from all possible directions. Therefore, the VDD model⁸ for polycrystalline growth that predicts $1/z \approx 0.4$ appears to be a better description of the underlying physics for $P \rightarrow 0$. In fact, when mass transport among crystals is hindered in our model, the competition among growing crystals is dominated by the highest crystals in an almost deterministic way approaching the conditions of VDD model.

In conclusion, our simple off-lattice model for the growth of polycrystalline materials stresses the importance of intracrystalline and intercrystalline surface mass transport, a topic which has been neglected so far in the theory of growth processes. Our model also demonstrates that scale-dependent growth exponents can be found depending on the heights of the energy barriers at crystal boundaries and step-edges. This fact explains the scale-dependent growth exponents for the growth of polycrystalline materials.

This work was financially supported by the Consejo Nacional de Investigaciones Científicas y Técnicas, CONICET (PIA 7283/97, PIP 014/97, and PIA 6456/97), the Universidad Nacional de La Plata, Fundación Antorchas, Argentina, and the Volkswagen Foundation (Germany). This work was also carried out within the framework of the CONICET–Consejo Superior de Investigaciones Científicas (Spain) cooperation agreement.

- *Visiting researcher from Instituto de Ciencia de Materiales de Madrid (CSIC), Cantoblanco, 28049 Madrid, Spain.
- ¹A. L. Barabasi and H. E. Stanley, in *Fractal Concepts in Surface Growth* (Cambridge University Press, Cambridge, 1995), and references therein.
- ²F. Family and T. Vicsek, *J. Phys. A* **18**, L75 (1985).
- ³J. H. Jeffries, J.-K. Zuo, and M. M. Craig, *Phys. Rev. Lett.* **76**, 4931 (1996).
- ⁴L. Vázquez, R. C. Salvarezza, P. Herrasti, P. Ocón, J. M. Vara, and A. J. Arvia, *Surf. Sci.* **345**, 17 (1996).
- ⁵L. Vázquez, R. C. Salvarezza, P. Herrasti, P. Ocón, J. M. Vara, and A. J. Arvia, *Phys. Rev. B* **52**, 2032 (1995).
- ⁶G. Palasantzas and J. Krim, *Phys. Rev. Lett.* **73**, 3564 (1994).
- ⁷L. Vázquez, R. C. Salvarezza, E. Albano, A. J. Arvia, A. Hernández Creus, R. A. Levy, and J. M. Albella, *Adv. Mater.* **4**, 89 (1998).
- ⁸A. Van der Drift, *Philips Res. Rep.* **22**, 267 (1967); J. M. Thijsen, *Phys. Rev. B* **51**, 1985 (1995).
- ⁹D. Wolf and J. Villain, *Europhys. Lett.* **13**, 389 (1990).
- ¹⁰Z.-W. Lai and S. Das Sarma, *Phys. Rev. Lett.* **66**, 2348 (1991).
- ¹¹Z. Zhang, J. Detch, and H. Metiu, *Phys. Rev. B* **48**, 4972 (1993); P. Smilauer and D. Vvedenski, *ibid.* **52**, 14 263 (1995).
- ¹²C. Tang, S. Alexander, and R. Bruinsma, *Phys. Rev. Lett.* **64**, 772 (1990).
- ¹³J. M. Thijssen, H. J. F. Knops, and A. J. Dammers, *Phys. Rev. B* **45**, 8650 (1992).
- ¹⁴Y. Li and A. E. DePristo, *Surf. Sci.* **351**, 189 (1996).
- ¹⁵H. Martin, A. Hernandez Creus, P. Carro, R. C. Salvarezza, and A. J. Arvia, *Langmuir* **13**, 100 (1997).
- ¹⁶J. H. Yao and H. Guo, *Phys. Rev. E* **47**, 1007 (1993).